Development of a high-pressure Ti-Mn based hydrogen storage alloy for hydrogen compression

Nayebossadri, Shahrouz; Book, David

DOI:
10.1016/j.renene.2019.05.052

Document Version
Peer reviewed version

Citation for published version (Harvard):
Nayebossadri, S & Book, D 2019, 'Development of a high-pressure Ti-Mn based hydrogen storage alloy for hydrogen compression', *Renewable Energy*, vol. 143, pp. 1010-1021.
https://doi.org/10.1016/j.renene.2019.05.052

Accepted Manuscript

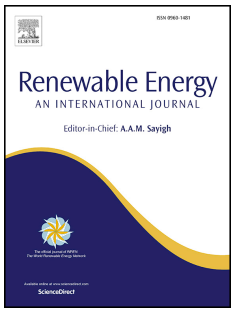

Development of a high-pressure Ti-Mn based hydrogen storage alloy for hydrogen compression

Shahrouz Nayebossadri, David Book

PII: S0960-1481(19)30712-8

DOI: https://doi.org/10.1016/j.renene.2019.05.052

Reference: RENE 11644

To appear in: *Renewable Energy*

Received Date: 8 November 2018

Revised Date: 12 April 2019

Accepted Date: 13 May 2019

Please cite this article as: Nayebossadri S, Book D, Development of a high-pressure Ti-Mn based hydrogen storage alloy for hydrogen compression, *Renewable Energy* (2019), doi: https://doi.org/10.1016/j.renene.2019.05.052.

Development of a high-pressure Ti-Mn based hydrogen storage alloy for hydrogen compression

Shahrouz Nayebossadri and David Book
School of Metallurgy and Materials, University of Birmingham,
Edgbaston, Birmingham, B15 2TT, UK

Abstract

This work focuses on the selection and development of high-pressure Ti-Mn based alloy for a domestic 2-stage Metal Hydride Hydrogen Compressor (MHHC) capable of compressing hydrogen from 15 bar to over 350 bar with a maximum operating temperature of 130 °C. Thermodynamic, kinetics and hydrogen storage characteristics of Ti-Mn based alloy were shown to be very sensitive to the alloy's composition. Stability of the hydride phase could be significantly reduced by increasing the Mn content of the alloy and contracting the C14 Laves phase unit cell volume, therefore meeting the required thermodynamic for the target MHHC. The structure and hydrogen capacity of the alloy remained almost constant even after 1000 hydrogen absorption and desorption cycles at room temperature. A significant reduction in the hydrogen absorption plateau slope of the modified high-pressure alloy was achieved by increasing the C14 Laves phase proportion. As a result, effective improvement in the hydrogen sorption kinetics of the modified alloy was observed with most of the hydrogen ab/desorbed in less than 5 min. Although compositional modification showed to be beneficial for lowering the hydrogen absorption plateau slope in high-pressure alloys, the level of hysteresis seemed to be mainly dominated by the alloys thermodynamic.

Keywords**:** *metal hydrides, hydrogen compression, Ti-Mn based alloys, C14 Laves phase*

1. Introduction

The Thermochemical properties of metal hydrides extend their application, beyond just a hydrogen storage medium, to those where a secondary effect such as gas compression, heat pumping or heat generation is important [1]. For example, the application of metal hydrides for gas compression was reported since the early 1970's [2,3], where the temperature dependence of hydride formation plateau pressure was used to compress hydrogen. Also, there has been significant interests in metal hydrides as heat pumps for heating/cooling and heat transformer systems [1].

Development of high-pressure hydrogen storage tanks for fuel cell vehicles [4], has generated the need for an efficient and reliable hydrogen compression method. Metal Hydride Hydrogen Compressors (MHHCs) can be coupled to low-pressure hydrogen sources such as hydrogen electrolysers to produce high-pressure hydrogen. In MHHCs hydrogen interacts with a hydride forming metal, alloy or intermetallic compound at low pressure and temperature to form a metal hydride. Subsequently, an increase in the metal hydride temperature, increases the hydrogen absorption equilibrium pressure allowing hydrogen to be released at higher pressures, the level of which depends on the particular thermodynamic properties of the metal hydride [5,6]. The hydrogen absorption and desorption process are repeated in MHHCs via a cyclic temperature swing operation to produce high-pressure hydrogen [1]. A thorough review of the MHHCs operation and the process requirements was given by Lototskyy et al. [7].

Depending on the required hydrogen pressure and the operation temperature, a single stage or a multistage MHHC can be designed [7]. Specific MHHC's operational parameters (such as maximum hydrogen pressure, hydrogen delivery rate, working temperature range)

can be scaled to meet user requirements. Besides scalability, MHHCs offer a number of advantages such as simplicity in design and operation, the absence of moving parts, possibility of exploiting waste heat, safety, reliability and silent operation making them interesting alternatives to mechanical compressors or more recently developed alternatives such as electrochemical and ionic liquid hydrogen compressors [7,13,14]. Although recent techno-economic analyses [15,16] predicted only a marginal lower capital cost for MHHCs compared to the mechanical compressors, MHHCs suggested to benefit from the significantly lower operation and maintenance costs with the possibility to achieve even more operational cost reduction by using waste heat. Several cost reduction and performance improvement methods for MHHCs are also proposed and the economic feasibility of the large-scale MHHCs are demonstrated for specific systems [16,17].

Materials selection is a crucial element in the MHHCs design as efficient performance of MHHCs strongly depends on the properties of the selected hydrides. The possibility of modifying metal hydrides properties is challenging due to the strict material requirements imposed by MHHCs, such as appropriate thermodynamic properties to achieve the required hydrogen compression ratio within the available working temperature, high reversible hydrogen capacity, fast kinetics, low plateau slope and low hysteresis. In addition, the selected materials should show tolerance to impurity gases, retain the desired hydrogen storage properties during numerous cycles and offer scalability at an affordable cost [7,18].

The ability to modify the thermodynamic properties of transition metal AB_2 alloys makes them appealing hydrogen storage materials. As a result, Laves phase AB_2 intermetallic alloys with extended compositional homogeneity ranges which crystallise in cubic ($MgCu_2$, C15) or hexagonal ($MgZn_2$, C14 and $MgNi_2$, C36) type structures [19] have been studied for high-

pressure hydrogen compression applications.. Deviations from AB_2 stoichiometry are associated with the occurrence of vacancies in the lattice, substitution of substoichiometric atom positions by super stoichiometric atoms in the structure, and occupation of interstitial sites by super stoichiometric atoms [20,21]. Moreover, additional alloying elements can be readily substituted on one or both atomic sites in most Laves phases [22].

Ti-Mn based AB_2 type Laves phase alloys are of particular interests as materials for hydrogen compression application as they offer acceptable hydrogen storage capacity at room temperature (~2 wt%), good hydrogen ab/desorption kinetics, good cycling properties, easy activation and low cost. However, these alloys suffer from poor plateau characteristics at desirable working pressures due to the sloping plateau and a relatively large hysteresis [23–26]. The effects of varying the Ti/Mn content and transition metals substitutions (multi-component alloys) on the structure, hydrogen capacity, plateau pressures, hydrogen ab/desorption kinetics and cyclic stability of the Ti-Mn based Laves phase have been investigated [27,28]. It was noted [27,29] that Ti-Mn Laves phase alloys with Ti concentrations above 36 at.% can readily absorb hydrogen at room temperature without a requirement for any activation process. However, the amount of desorbed hydrogen was reduced for Ti content above 40 at.% due to the formation of very stable TiH_2 phase. Optimum hydrogen storage performance was reported by enhancing the stability of the C14 Laves phase during hydrogenation and adjusting lattice constants of the C14 Laves phase in off-stoichiometry $TiMn_{1.5}$ alloy [17].

In other studies, the hydrogen storage properties of the Ti-Mn based multi-component alloys were observed to be greatly influenced by the substitution of transition metals and variation of the alloy's composition [30,31]. In particular, Ti-V-Mn alloys which mainly

consist of C14 Laves and BCC phases were proposed as suitable candidates for high-pressure application due to the high hydrogen storage capacity, fast kinetics, good cycling properties and easy activation [24,25]. Varying the alloy composition and the elemental substitution allowed the properties of Ti-V-Mn alloys to be tailored, although beneficial effects of these modifications appear difficult to predict. For example, whilst increasing V content improved the activation process and encouraged the formation of BCC phase, its substitution for Ti or Mn led to opposite effects on the hydrogen absorption plateau pressure [23,25,31–33]. Hydrogen storage properties of multi-component Ti-V-Mn based alloys were also studied following the substitution of transition metals either in A or B sites [23,31,32,34–39]. It was noted that [32,38,39] partial substitution of Ti by Zr, could increase the hydrogen capacity whilst lowering the hydrogen absorption plateau pressure. Substitution of other transition metals such as Cu, Cr, Ni, Fe, Mo, Nb, and Ta led to improved plateau slope and hysteresis, but their primary effect was on the hydrogen absorption plateau pressure [23,31,37,39]. Whilst, the Mn content seemed to be a dominant factor in determining the hydrogen absorption plateau pressure [38], transition metals could also effectively change the hydrogen absorption capacity and the plateau pressure of multi-component alloys by varying the C14 Laves phase cell volume [31,32,35,39]. In general, a decrease in hydrogen absorption plateau pressure can be expected by increasing the C14 Laves phase unit cell volume due to the creation of larger interstitial sites for hydrogen occupation, enhancing the hydride stability [40,41]. Hence, the structure and thermodynamic properties of these alloys appear to be closely related to their composition and therefore, compositional modification should be an effective method for modifying and tailoring their hydrogen storage properties.

In this study, we focused on the development of high pressure Ti-Mn based alloy as a 2nd stage material for a domestic two-stage MHHC (compressing 600g hydrogen in 10 h from an inlet pressure of 15 bar to 350 bar within a working temperature range of room temperature to 130 °C) suitable for overnight refuelling the hydrogen vehicles. This will supply enough hydrogen for distance traveled (40 miles) by average car owners a day [42].

To accelerate the modification process, we initially altered the composition of the commercially available Ti-Mn based alloy and then fabricated the modified alloy from the elements. Considering a careful balance of the substituting elements, the effects of compositional modification on thermodynamics, kinetics, plateau characteristics and cyclic stability of the modified alloy are demonstrated and discussed.

2. Materials and Methods

Ti-Mn based Laves phase hydrogen storage grade alloy was purchased from Sigma Aldrich. Hydralloy C was purchased from GfE. Elemental Ti (sponge, 99.95%), V (pieces, 99.7%), Mn (pieces, 99.9%), Zr (sponge 99.5%), Cr (pieces, 99.995%), Fe (pieces, 99.99%) and Ni (powder, 99%) were purchased from Alfa Aesar. Modified alloys were prepared by arc melting on a water-cooled copper crucible in an argon atmosphere which was purified by melting a sacrificial oxygen getter before melting the alloys. Alloys were pressed into pellets using an ATLAS automatic uniaxial press to produce a 2 g charge and arc melting current was kept at 70 A to minimise the risk of losing elements during the arc strike. Each alloy was rotated and melted at least three times to ensure the homogeneity. No heat treatment was performed on the fabricated alloys and they were crushed to a particle size of less than 50 μm.

Pressure Compositional Isotherm (PCI) measurements were performed under high purity hydrogen (99.99% from BOC) using a volumetric Sieverts-type system (Hiden Isochema HTPS-2). In-situ activation sequence was performed for all alloys (at least 5 times) before PCI measurement by heating the alloy to 300 °C and then admitting 100 bar H_2. Alloys were kept at this pressure for 4 h whilst cooling down to room temperature and vacuumed to approximately 10^{-6} mbar at the end of the sequence. Hydrogen absorption kinetic measurements were performed using the same system by dosing hydrogen and monitoring the pressure decrease in the dose volume. A static overpressure of 1.5 times higher than the plateau pressure of each alloy was applied to ensure enough driving force for hydrogen absorption and fully hydrogenating the alloy. The hydrogen pressure was rapidly removed by opening the dose volume to the vent before measuring the hydrogen desorption kinetic and then monitoring the pressure increase in the dose volume.

Cyclic hydrogen ab/desorption measurement was performed on the activated sample between 0.5 and 70 bar H_2 pressure at room temperature using another volumetric Sieverts-type system built by the Hydrogen Materials Group at the University of Birmingham.

Room temperature X-Ray Diffraction (XRD) measurements were performed using a Bruker D8–Advanced diffractometer with monochromatic CuKα radiation (λ = 1.54056 Å). The XRD data was refined via a pseudo–Rietveld method with TOPAS Academic software [43] using published crystallographic information files (.cif) obtained from the Inorganic Crystal Systems Database [44].

Alloys composition were analysed by a Joel 6060 Scanning Electron Microscope (SEM) equipped with an INCA 300 Energy Dispersive Spectrometer (EDS).

3. Results

3.1. Modification of commercial Ti-Mn based alloy

The XRD pattern of the commercial Ti-Mn based alloy is shown in Fig. 1. The alloy contains C14 Laves phase and FCC oxide phase (A_3B_3O) where A=Ti and Zr and B=Mn and V. Precipitation of η-carbide type oxide A_3B_3O, was reported in as-cast $Zr_{0.75}Ti_{0.25}MnV$ alloy [36] and also observed in a number of studies on other Ti-Mn based alloys [24,25,33,37]. The detrimental effect of oxygen on the microstructure and therefore homogeneity of the C14 Laves phase [28] can substantially alter the hydrogen absorption properties of the alloy. Structural refinement provides (Alloy 1 in Table 1) a phase abundance of 93% and 7% for the C14 Laves and FCC oxide phases respectively. The C14 Laves phase is the major hydrogen absorbing phase in this alloy hence the volume fraction should be maximised due to its favourable hydrogen absorption properties [29,35,36].

Compositional analysis by EDS, given in Table 1, indicates that the alloy contains a small amount of other substituting elements for A (Zr) and B (V, Fe, Cr) sites but their presence at such a scale should not encourage the formation of any new phase/s. In fact, up to 26 at.% V was reported [20,32] to dissolve in the $TiMn_2$ C14 Laves phase without causing any structural changes. The large structural homogeneity region observed in Laves phase compounds originates from the capability of substitutional elements to occupy the atomic crystallographic positions of typical primary phase constituents [34]. Hence, thermodynamic and kinetic properties of Laves phase compounds may be tuned by the development of multicomponent off-stoichiometry (B/A=2±x) alloys without inducing changes in the Laves phase structure.

The interactions between commercial Ti-Mn based alloy and hydrogen at various temperatures are shown by PCI measurements in Fig. 2. A single plateau for hydrogen absorption can be observed with the plateau slope increases with increasing the temperature. The room temperature slope factor of this alloy, which is given in Table 2, indicates a wide range of pressure (approximately 20-45 bar) is required to fully hydrogenate the alloy. Alloys with sloping plateau are not well suited to MHHCs as it can significantly reduce the hydrogen compression ratio [7]. In addition, a large hysteresis is usually observed in Laves phase alloys containing Mn [20]. Similarly, a relatively large hysteresis can be observed for this alloy (Table 2) implying additional energy consumption and reduced hydrogen compression efficiency in MHHC [7].

Room temperature hydrogen absorption and desorption kinetics of the commercial Ti-Mn based alloy is shown in Fig. 3. The hydrogen absorption kinetic for some AB_2 alloys were measured [45–47] and showed to be a function of pressure, temperature and the composition of the alloy. While the first 20% of hydrogen uptake is rapid in Alloy 1, a notable reduction in the rate of hydrogen absorption can be seen at this point, causing incomplete hydrogen absorption even after a prolonged hydrogen exposure. Furthermore, 60% of hydrogen can be rapidly (less than 2 min) released from the alloy after which the rate of hydrogen desorption becomes very slow.

The thermodynamic parameters for metal hydride formation can be estimated by the van't Hoff equation [7,48,49]:

$$\ln P = \frac{\Delta H}{RT} - \frac{\Delta S}{R} \quad (1)$$

Where *P* is the equilibrium pressure (atm) defined by the mid-point of the PCI plateau pressure between two inflection points, ΔH and ΔS are enthalpy and entropy changes of the

hydrogen ab/desorption reactions, T is absolute temperature and R is the gas constant. Using the van't Hoff equation, ΔH and ΔS values of 25.8 kJ/mol H_2 and 110 J/Kmol were estimated (Table 2) for hydrogen desorption from commercial Ti-Mn based alloy. This implies a maximum hydrogen desorption pressure of slightly over 230 bar at the highest operation temperature (130 °C) of the target MHHC. Hence, the thermodynamics of the alloy should be modified to form a less stable hydride (with a higher plateau pressure) capable of delivering the intended higher hydrogen pressure (350 bar) at the maximum operating temperature.

Compositional modifications of the alloy were performed by elemental additions to the as-received Ti-Mn based alloy and the EDS results of the modified alloys are given in Table 1. Although compositional modifications may favour the formations of off-stoichiometry alloys, the structure of the alloys remains same except that Alloys 2 and 4 containing a small amount of BCC phase due to the increased V content [23–25]. Also, notable changes in the C14 Laves phase unit cell volume of the modified alloys can be observed in Table 1 following the compositional modifications. PCI measurements of the modified alloys (Supporting Information Fig. S1-S24 for PCI curves and XRD patterns) show substantial changes in the hydrogen absorption plateau pressures(Table 2) as a result of compositional modifications. An almost linear relationship between the C14 Laves phase unit cell volume and the plateau pressure of the studied alloys can be observed in Fig. 4, confirming the significant effect of C14 Laves phase unit cell volume on the thermodynamics of the alloys [40,41]. Thermodynamics, kinetics and PCI characteristics of the modified alloys are given in Table 2. Stability of the hydride phase seems to be decreased in Alloys 8 to 13, indicating the primary role of the Mn to destabilise the hydride phase [20,34,38,50]. Despite a lower hydrogen

capacity of the Alloy 11 compared to the commercial alloy, it can be a suitable alloy for the high-pressure stage of the target MHHC because of its acceptable thermodynamic, fast kinetic and the lowest plateau slope observed amongst the studied alloys. In addition, it was noted that the activation process is significantly easier in this alloy possibly due to a small amount of V addition [23]. Also, it seems that thermodynamic destabilisation in Alloys 8 to 13 leads to an increased hysteresis (Table 2). This may be due to an increased level of strain during hydrogenation as a result of the contraction in C14 Laves phase unit cell volume [26] and therefore hysteresis and hydrogen capacity seem to be compromised for high-pressure alloys [30].

3.2 Modified alloy

To ensure the compositional uniformity and control of the scale-up process, the modified alloy (Alloy 14) was synthesised from elements according to the composition of Alloy 11. The XRD pattern of the Alloy 14 is shown in Fig. 5(a). The C14 Laves phase is the main phase observed with a small peak for the A_3B_3O phase. In fact, structural refinement (Table 1) indicates that the proportion of C14 Laves phase in the Alloy 14 is approximately 99%. Minimising the oxide phase is particularly useful to promote the C14 Laves phase homogeneity and hydrogen absorption properties of the alloy. Compositional analysis of the Alloy 14 is given in Table 1, which indicates an increase in the B/A ratio (2.26) compared to Alloy 11. The increased B/A ratio of the Alloy 14 seems to slightly reduce the C14 Laves phase unit cell volume compared to the Alloy 11, possibly due to an increased Mn content at the expense of Ti.

PCI measurements (Fig. 6) show a single plateau for hydrogen absorption at various temperatures for the Alloy 14. The hydrogen absorption characteristics of the Alloy 14 are

also given in Table 2. While the room temperature slope factor of this alloy is lower compared to Alloy 11, it has a slightly higher hysteresis value due to lower thermodynamic stability (Table 2). The hydrogen capacity of Alloy 14 seems to be improved compared to Alloy 11, probably a result of less oxide phase content and the introduction of fewer impurities when synthesising the alloy from the elements. In addition, room temperature hydrogen absorption and desorption kinetics of the Alloy 14 is shown in Fig. 7. Similar to the Alloy 11 rapid rates for 80% hydrogen absorption (~3min) and desorption (less than 2 min) can be seen in the current experimental results.

Structural stability of the alloy is also crucial during the extended cyclic operation of MHHCs. Degradation of the alloy properties under high purity hydrogen is likely to happen as a result of intermetallic disproportionation which is a function of temperature and pressure [7]. The interaction between the alloying elements and hydrogen may be thermodynamically conducive to the formation of stable binary hydrides leading to lower hydrogen capacity. Nevertheless, a promising cyclic stability was reported for the AB_2 alloys after an extended cycling under hydrogen [51]. The reversible hydrogen storage capacity of the Alloy 14 as a function of hydrogen absorption/desorption cycles at room temperature is given in Fig. 8(a and b). While there is not a noticeable change in the hydrogen storage capacity of the Alloy 14 until 265 cycles, a slow reduction in the hydrogen storage capacity of the alloy is observed after this point and continues up to 655 cycles, which equals to 9% reduction in the overall hydrogen storage capacity (Fig. 8(b)). The hydrogen storage capacity of the alloy seems to become stable after 655 cycles and no further reduction can be observed up to 1007 cycles. The structure of the alloy after cycling is shown in Fig. 5(b). It is clear that the alloy retains its C14 Laves phase structure after cycling and the formation of

any new phase can not be observed. The small reduction in the hydrogen capacity observed in Fig. 8(b), may originate from the impurities in the gas stream or limited pulverisation of the alloy.

The speculative operation condition of the developed high-pressure alloy (Alloy 14) was derived from thermodynamic values listed in Table 2. Figure 9 shows the operating conditions for the target MHHC when the developed high-pressure alloy (2^{nd} stage) is combined with an alloy having a lower hydride formation pressure (1^{st} stage). The proposed 1^{st}-stage alloy (Hydralloy C, Supporting Information Fig. S25) can be fully hydrogenated under an inlet pressure of 15 bar. Increasing the temperature of the 1^{st}-stage alloy to 100 °C will supply a hydrogen pressure of approximately 70 bar, which is more than 1.5 times higher than the plateau pressure of the Alloy 14. This will ensure sufficient driving force at room temperature for the full hydrogenation of the Alloy 14 and therefore maximising the hydrogen productivity of the MHHC. The outlet hydrogen pressure of the MHHC will exceed 350 bar if the temperature of the 2^{nd}-stage alloy increases to 130 °C (compression ratio > 23), hence meeting the operation temperature of the target MHHC.

Alloy 14 which it's A-element is mainly consist of Ti can also offer a cost advantage over the AB_5 alloys that are relying on expensive rare earth elements. In fact, the alloy composition allows the use of low-cost ferrovanadium instead of expensive pure vanadium. Nevertheless, the material cost in MHHCs is estimated [13] to be only about 2% of the overall cost and therefore not the main criterion in the selection of metal hydride materials compared to other important thermodynamics, kinetics and PCI characteristics.

4. However, the mass production of the developed alloy in this study may be difficult as the alloy properties are very sensitive to the composition. Conventional melting

techniques may not be suitable for the mass production of this alloy due to the high melting point of the constituting element and the introduction of impurities. The author has successfully fabricated approximately 1 kg batches of the Alloy 14, using a Plasma furnace. Great metallurgical care was required to avoid the introduction of impurities and loss of Mn to achieve reproducible thermodynamics and kinetics properties. The appropriate melting process was established by two trail runs before melting the 1st batch with no further modification required afterward (Supporting Information, Fig. S26). **Discussion**

The present results show hydrogen storage properties of the modified alloys are strongly depending on alloy composition and structure. It has been proposed elsewhere that an increase in the B/A stoichiometric ratio of the AB_2 alloys can increase the hydrogen sorption equilibrium pressure as a result of the contraction in the unit cell volume [52,53]. In fact, a direct relationship between the size of tetrahedral interstitial sites and thermodynamic properties of hydride formation in intermetallic compounds was proposed by Lundin et al. [40]. It was shown in the present work that increasing the Mn content of the alloy is the most effective method to destabilise the hydride phase by decreasing the C14 Laves phase unit cell volume. The contraction can be brought about by creating vacancies in the A sites and substitution of Mn for Ti/Zr in the A sites, both reducing in the C14 Laves phase unit cell volume. Alternatively, changes in the hydrogen sorption equilibrium pressure were also suggested to originate from electronic structure [39,46,47,52] and chemical affinity [35] of the alloys to hydrogen. Changes in the average electron density may influence the phase structure of the Laves phase and therefore, affecting the hydrogen sorption equilibrium pressure of the alloy. All the studied alloys retained their C14 structure, which may indicate

that no significant changes in the electronic structure of the alloys have occurred. However, the impact of variation in chemical affinity on the hydrogen sorption equilibrium pressure seems to be a less significant factor. For example, Alloys 5-7 were modified by small additions of Ni, Cr and Fe, which have less chemical affinity to hydrogen compared to Mn used to modify Alloy 8, but form hydride phase at lower hydrogen absorption plateau pressures ($\Delta H_{formation}$ are Ni: 9.2 kJ/mol H, Cr: 39.6 kJ/mol H, Fe: 30.3 kJ/mol H , and Mn: -1.9 kJ/mol H [54,55]). Hence, it seems that hydrogen sorption equilibrium pressure in these alloys is mainly dominated by the variation in the Laves phase unit cell volume.

Many studies [7,24,50,53,56] indicate chemical inhomogeneity as the origin of slopping plateaux during hydrogen sorption process. Chemical inhomogeneity can arise from the level of complexity of the alloy structure in terms of the number of existing phases, types and concentration of the modifying elements, compositional inhomogeneity and impurities. The overall relationship between the hydrogen absorption plateau slope and the C14 Laves phase concentration for the alloys containing two phases (C14 and A_3B_3O) is shown in Fig. 10. The slope of the hydrogen absorption plateau pressure generally seems to decline by increasing the C14 Laves phase proportion in the alloys. The formation of C14 Laves single phase region can be encouraged in alloys with high Mn content [36] and also an accurate control over the synthesising process, leading to a lower hydrogen absorption plateau slope. In addition, increasing the C14 Laves phase proportion seems to be beneficial in improving the hydrogen sorption kinetics and capacity (Table 1 and 2), according to the known properties of the C14 Laves phase [27,35].

Also, the strong dependency of the hydrogen absorption plateau slope on the type of the modifying elements can be seen in Fig. 10. For example, Alloys (1), (5), (7) and (11) possess

different slope values, while containing an equal amount of C14 Laves phase. Modification of the as-received alloy with a small amount of Ni in the Alloy 5 and Fe in the Alloy 7 seems to increase the hydrogen absorption plateau slope, whereas addition of V and Mn in the Alloy 11 results in a notable reduction in the hydrogen absorption plateau slope. The effect of the modifying elements on the hydrogen sorption plateau slope has been described [47,57,58] using the local chemical model developed by Ivey et al. [59]. The Laves phase hexagonal structure is capable of accommodating hydrogen in seven different types of tetrahedral interstitial sites despite having different affinity to hydrogen [34]. The introduction or substitution of modifying elements in either A or B sites can encourage the formation of other interstitial sites with different local chemical environments and therefore broaden the required pressure range for hydrogen absorption. For example, the introduction of Ti into the B sites can create a series of interstitial sites rich in Ti, such as Ti(2)Ti(2), Ti(2)TiB, and TiTi(3), showing different affinities to hydrogen [57]. Increasing the number of interstitial sites with the different local chemical environment will result in a higher hydrogen sorption plateau slope. Thus, off-stoichiometry alloys, where modifying elements are substituted in either A or B interstitial sites are expected to represent higher plateau slopes compared to the stoichiometric alloy. Nevertheless, such a trend cannot be observed in all our modified off-stoichiometry alloys. In fact, Alloy 14 with B/A ratio of 2.16 owns the lowest hydrogen absorption plateau slope among the modified alloys. It may imply that a change in the local chemical environment is not the only factor controlling the hydrogen sorption plateau slopes. Interstitial site occupations in metal hydrides have also been predicted using geometrical models [60], defining the minimum interstitial size to accommodate H atoms and the required minimum distance between two H occupied sites.

Determining the dimensions of the interstitial sites in the modified off-stoichiometry alloys may assist in predicting the interaction between H and specific interstitial sites. We believe, if the magnitude of energy difference for H occupation in the interstitial sites is minimised, a decline in the hydrogen sorption plateau slopes may be expected even for off-stoichiometry alloy.

Hysteresis has been observed for many metal hydrides systems and its origin has been related to the plastic deformation of the lattice as a result of strain during the hydrogenation, defects and dislocation formation [7,59,61]. Fig. 11 shows the relation between the mid-plateau pressure and hysteresis of the studied alloys. The overall trend suggests an elevation in hysteresis by increasing the plateau pressure. The effect of the modifying elements on the level of hysteresis seems to be less significant compared to the effect of plateau pressure, indicating the possibility of a substantial contribution from lattice strain on the level of hysteresis as the lattice size decrease. However, It should be noted that the level of impurities, the process history of alloy and the test conditions have been suggested to influence the hysteresis in metal hydrides [59]. Therefore, it seems less likely to reduce the hysteresis, particularly for the high-pressure alloys, through compositional modification as it mainly arises from the thermodynamics of the alloys.

5. Conclusions

A high-pressure Ti-Mn based alloy was developed to be employed in the high-pressure stage of a 2-stage MHHC capable of compressing hydrogen from an inlet pressure of 15 bar to above 350 bar, while the operating temperature not exceeding 130 °C. Compositional modification appeared to be an effective method to alter the thermodynamics, kinetics and hydrogen sorption characteristics of the alloy. An optimum off-stoichiometric composition

($Ti_{30}V_{15.8}Mn_{49.4}(Zr_{0.5}Cr_{1.1}Fe_{2.9})$) for a high-pressure alloy was selected and synthesised from the elements. Structural homogeneity of this alloy was enhanced by increasing C14 Laves phase proportion as the main hydrogen absorption phase. The unit cell volume of the C14 Laves phase of this alloys was reduced compared to the commercial alloy (163.95 to 163.5 $Å^3$), leading to acceptable thermodynamics for the operation of the desired MHHC. Increasing the Mn content of the alloy appeared to be the most effective method to decrease the C14 Laves phase unit cell volume. In addition, enhanced structural homogeneity had a notable effect on improving the activation process, hydrogen ab/desorption kinetics and PCI characteristics of the alloy. In fact, more than 80% of hydrogen could be ab/desorbed from the alloy in less than 5 min. This alloy showed the least plateau slope among the studied alloys, possibly due to the increased C14 Laves phase proportion and minimising the energy difference between available interstitial sites for hydrogen occupation. Unlike the plateau slope, reducing the level of hysteresis through the compositional modification seems to be less likely for high-pressure alloys as the thermodynamics of the alloy seems to impact the hysteresis most. Cyclic property of the modified alloy was monitored for more than 1000 cycles of hydrogen absorption and desorption at 70 and 0.5 bar respectively. Only 9% reduction in hydrogen capacity was observed between 265 and 655 cycles where the capacity remained unchanged until the end of the measurements. Structural analyses before and after cyclic measurements revealed the capability of the alloy to retain its C14 Laves phase structure with no sign of degradation. The developed alloy will enable more efficient operation of MHHCs for high-pressure hydrogen compression due to the desired PCI properties and durability.

Acknowledgments

Support from the EPSRC Engineering Safe and Efficient Hydride-based Technologies (EP/K021117/1) and STFC Early Career Award (ST/N002385/1) is gratefully acknowledged.

Authors would like to thank Professor David Grant, Professor Gavin Walker and Dr Alastair Stuart for their supports and guidance.

References:

1. Wipf H, Grabert H. Schober H. R. , Barnes R. G., Ross D. K., Vehoff H., D. P. *Hydrogen in metals III: properties and applications*; H.Wipf, Ed.; New York: Springer, 1997;

2. Reilly, J. J.; Holtz, A.; Wiswall, R. H. A New Laboratory Gas Circulation Pump for Intermediate Pressures. *Rev. Sci. Instrum.* **1971**, *42*, 1485–1486, doi:10.1063/1.1684913.

3. van Mal, H. H. A LaNi5-Hydride Thermal Absorption Compressor for a Hydrogen Refrigerator. *Chemie Ing. Tech. - CIT* **1973**, *45*, 80–83, doi:10.1002/cite.330450207.

4. Jorgensen, S. W. Hydrogen storage tanks for vehicles: Recent progress and current status. *Curr. Opin. Solid State Mater. Sci.* **2011**, *15*, 39–43, doi:10.1016/j.cossms.2010.09.004.

5. Bellosta von Colbe, J.; Ares, J. R.; Barale, J.; Baricco, M.; Buckley, C.; Capurso, G.; Gallandat, N.; Grant, D. M.; Guzik, M. N.; Jacob, I.; Jensen, E. H.; Jensen, T.; Jepsen, J.; Klassen, T.; Lototskyy, M. V.; Manickam, K.; Montone, A.; Puszkiel, J.; Sartori, S.; Sheppard, D. A.; Stuart, A.; Walker, G.; Webb, C. J.; Yang, H.; Yartys, V.; Züttel, A.; Dornheim, M. Application of hydrides in hydrogen storage and compression: Achievements, outlook and perspectives. *Int. J. Hydrogen Energy* **2019**, *44*, 7780–7808, doi:10.1016/j.ijhydene.2019.01.104.

6. Karagiorgis, G.; Christodoulou, C. N.; von Storch, H.; Tzamalis, G.; Deligiannis, K.; Hadjipetrou, D.; Odysseos, M.; Roeb, M.; Sattler, C. Design, development, construction and operation of a novel metal hydride compressor. *Int. J. Hydrogen Energy* **2017**, *42*, 12364–12374, doi:10.1016/j.ijhydene.2017.03.195.

7. Lototskyy, M. V.; Yartys, V. A.; Pollet, B. G.; Bowman, R. C. Metal hydride hydrogen compressors: A review. *Int. J. Hydrogen Energy* **2014**, *39*, 5818–5851, doi:10.1016/j.ijhydene.2014.01.158.

8. Bhogilla, S. S.; Niyas, H. Design of a hydrogen compressor for hydrogen fueling stations. *Int. J. Hydrogen Energy* **2019**, doi:10.1016/j.ijhydene.2019.02.171.

9. Muthukumar, P.; Singh Patel, K.; Sachan, P.; Singhal, N. Computational study on metal hydride based three-stage hydrogen compressor. *Int. J. Hydrogen Energy* **2012**, *37*, 3797–3806, doi:10.1016/j.ijhydene.2011.05.104.

10. Madaria, Y.; Anil Kumar, E. Effect of heat transfer enhancement on the performance of metal hydride based hydrogen compressor. *Int. J. Hydrogen Energy* **2016**, *41*, 3961–3973, doi:10.1016/j.ijhydene.2016.01.011.

11. Muthukumar, P.; Kumar, A.; Raju, N. N.; Malleswararao, K.; Rahman, M. M. A critical review on design aspects and developmental status of metal hydride based thermal machines. *Int. J. Hydrogen Energy* **2018**, *43*, 17753–17779, doi:10.1016/j.ijhydene.2018.07.157.

12. Minko, K. B.; Bocharnikov, M. S.; Yanenko, Y. B.; Lototskyy, M. V.; Kolesnikov, A.; Tarasov, B. P. Numerical and experimental study of heat-and-mass transfer processes in two-stage metal hydride hydrogen compressor. *Int. J. Hydrogen Energy* **2018**, *43*, 21874–21885, doi:10.1016/j.ijhydene.2018.09.211.

13. Yartys, V. A.; Lototskyy, M.; Linkov, V.; Grant, D.; Stuart, A.; Eriksen, J.; Denys, R.; Bowman, R. C. Metal hydride hydrogen compression: recent advances and future prospects. *Appl. Phys. A* **2016**, *122*, 415, doi:10.1007/s00339-016-9863-7.

14. Kelly, N. A.; Girdwood, R. Evaluation of a thermally-driven metal-hydride-based hydrogen compressor. *Int. J. Hydrogen Energy* **2012**, *37*, 10898–10916, doi:10.1016/j.ijhydene.2012.04.088.

15. Stamatakis, E.; Zoulias, E.; Tzamalis, G.; Massina, Z.; Analytis, V.; Christodoulou, C.; Stubos, A. Metal hydride hydrogen compressors: Current developments and early markets. *Renew. Energy* **2018**, *127*, 850–862, doi:10.1016/j.renene.2018.04.073.

16. Corgnale, C.; Sulic, M. Techno-Economic Analysis of High-Pressure Metal Hydride Compression Systems. *Metals (Basel).* **2018**, *8*, 469, doi:10.3390/met8060469.

17. Lototskyy, M.; Klochko, Y.; Davids, M. W.; Pickering, L.; Swanepoel, D.; Louw, G.; Van Der Westhuizen, B.; Chidziva, S.; Sita, C.; Bladergroen, B.; Linkov, V. Industrial-scale metal hydride hydrogen compressors developed at the South African Institute for Advanced Materials Chemistry. *Mater. Today Proc.* **2018**, *5*, 10514–10523, doi:10.1016/j.matpr.2017.12.383.

18. Muthukumar, P.; Prakashmaiya, M.; Srinivasamurthy, S. Experiments on a metal hydride based hydrogen compressor. *Int. J. Hydrogen Energy* **2005**, *30*, 879–892, doi:10.1016/j.ijhydene.2004.09.003.

19. Baumann, W.; Leineweber, A.; Mittemeijer, E. J. The kinetics of a polytypic Laves phase transformation in TiCr2. *Intermetallics* **2011**, *19*, 526–535, doi:10.1016/j.intermet.2010.11.027.

20. Mitrokhin, S. V. Regularities of hydrogen interaction with multicomponent Ti(Zr)–Mn–V Laves phase alloys. *J. Alloys Compd.* **2005**, *404–406*, 384–387, doi:10.1016/j.jallcom.2005.02.078.

21. Stein, F.; Palm, M.; Sauthoff, G. Structure and stability of Laves phases. Part I. Critical assessment of factors controlling Laves phase stability. *Intermetallics* **2004**, *12*, 713–720, doi:10.1016/j.intermet.2004.02.010.

22. Livingston, J. D. Laves-phase superalloys? *Phys. Status Solidi* **1992**, *131*, 415–423, doi:10.1002/pssa.2211310215.

23. Yu, X.; Xia, B.; Wu, Z.; Xu, N. Phase structure and hydrogen sorption performance of Ti-Mn-based alloys. *Mater. Sci. Eng. A* **2004**, *373*, 303–308, doi:10.1016/j.msea.2004.02.008.

24. Shibuya, M.; Nakamura, J.; Enoki, H.; Akiba, E. High-pressure hydrogenation properties of Ti–V–Mn alloy for hybrid hydrogen storage vessel. *J. Alloys Compd.* **2009**, *475*, 543–545, doi:10.1016/j.jallcom.2008.07.121.

25. Shibuya, M.; Nakamura, J.; Akiba, E. Hydrogenation properties and microstructure of Ti-Mn-based alloys for hybrid hydrogen storage vessel. *J. Alloys Compd.* **2008**, *466*, 558–562, doi:10.1016/j.jallcom.2007.11.120.

26. Liu, B.-H.; Kim, D.-M.; Lee, K.-Y.; Lee, J.-Y. Hydrogen storage properties of TiMn2-based alloys. *J. Alloys Compd.* **1996**, *240*, 214–218, doi:10.1016/0925-8388(96)02245-1.

27. Gamo, T.; Moriwaki, Y. Formation and properties of titanium-manganese alloy hydrides. *Int. J. Hydrogen Energy* **1985**, *1*, 39–47.

28. Bernauer, O. Topler, J. Noresus, D. Hempelmann, R. Richter, D. F U N D A M E N T A L S A N D PROPERTIES OF SOME Ti/Mn BASED LAVES PHASE HYDRIDES 0 . *Int. J. Hydrogen Energy* **1989**, *14*, 187–200.

29. Semboshi, S.; Masahashi, N.; Hanada, S. Effect of composition on hydrogen absorbing properties in binary TiMn2 based alloys. *J. Alloys Compd.* **2003**, *352*, 210–217, doi:10.1016/S0925-8388(02)01125-8.

30. Hagström, M. .; Vanhanen, J. .; Lund, P. . AB2 metal hydrides for high-pressure and narrow temperature interval applications. *J. Alloys Compd.* **1998**, *269*, 288–293, doi:10.1016/S0925-8388(98)00213-8.

31. Au, M.; Pourarian, F.; Sankar, S. G.; Wallace, W. E.; Zhang, L. TiMn2-based alloys as high hydrogen storage materials. *Mater. Sci. Eng. B* **1995**, *33*, 53–57.

32. Mitrokhin, S. .; Bezuglaya, T. .; Verbetsky, V. . Structure and hydrogen sorption properties of (Ti,Zr)–Mn–V alloys. *J. Alloys Compd.* **2002**, *330–332*, 146–151, doi:10.1016/S0925-8388(01)01469-4.

33. Pickering, L.; Li, J.; Reed, D.; Bevan, A. I.; Book, D. Ti-V-Mn based metal hydrides for hydrogen storage. *J. Alloys Compd.* **2013**, *580*, S233–S237, doi:10.1016/j.jallcom.2013.03.208.

34. Mitrokhin, S. V; Smirnova, T. N.; Somenkov, V. A.; Glazkov, V. P.; Verbetsky, V. N. Structure of (Ti,Zr)-Mn-V nonstoichiometric Lavas phases and (Ti0.9Zr0.1)(Mn0.75V0.15Ti0.1D2.8 deuteride. *J. Alloys Compd.* **2003**, *357*, 80–83.

35. Lee, H. H.; Lee, K. Y.; Lee, J. Y. The Ti-based metal hydride electrode for Ni-MH

rechargeable batteries. *J. Alloys Compd.* **1996**, *239*, 63–70, doi:10.1016/0925-8388(96)02276-1.

36. Huot, J.; Akiba, E.; Ishido, Y. Crystal structure of multiphase alloys (Zr, Ti)(Mn, V) 2. *J. Alloys Compd.* **1995**, *231*, 85–89.

37. Pickering, L.; Reed, D.; Bevan, A. I.; Book, D. Ti-V-Mn based metal hydrides for hydrogen compression applications. *J. Alloys Compd.* **2015**, *645*, S400–S403, doi:10.1016/j.jallcom.2014.12.098.

38. Dehouche, Z.; Savard, M.; Laurencelle, F.; Goyette, J. Ti-V-Mn based alloys for hydrogen compression system. *J. Alloys Compd.* **2005**, *400*, 276–280, doi:10.1016/j.jallcom.2005.04.007.

39. Xu, Y.-H.; Chen, C.-P.; Geng, W.-X.; Wang, Q.-D. The hydrogen storage properties of Ti–Mn-based C14 Laves phase intermetallics as hydrogen resource for PEMFC. *Int. J. Hydrogen Energy* **2001**, *26*, 593–596, doi:10.1016/S0360-3199(00)00124-5.

40. Lundin, C. E.; Lynch, F. E.; Magee, C. B. A correlation between the interstitial hole sizes in intermetallic compounds and the thermodynamic properties of the hydrides formed from those compounds. *J. Less-Common Met.* **1977**, *56*, 19–37, doi:10.1016/0022-5088(77)90215-6.

41. Nakano, H.; Wakao, S.; Shimizu, T. Correlation between crystal structure and electrochemical properties of C14 Laves-phase alloys. *J. Alloys Compd.* **1997**, *253–254*, 609–612, doi:10.1016/S0925-8388(96)03089-7.

42. Engineering Safe and Efficient Hydride-Based Technologies Available online: http://gow.epsrc.ac.uk/NGBOViewGrant.aspx?GrantRef=EP/K021117/1.

43. Coelho, A. Topas-Academic, Version 4.1, Coelho Software, Brisbane, Australia. **2007**.

44. Fletcher, D. A.; McMeeking, R. F.; Parkin, D. The United Kingdom Chemical Database Service. *J. Chem. Inf. Model.* **1996**, *36*, 746–749, doi:10.1021/ci960015+.

45. Manickam, K.; Grant, D. M.; Walker, G. S. Optimization of AB2 type alloy composition with superior hydrogen storage properties for stationary applications. *Int. J. Hydrogen Energy* **2015**, *40*, 16288–16296, doi:10.1016/j.ijhydene.2015.09.157.

46. Kandavel, M.; Ramaprabhu, S. Hydriding properties of Ti-substituted non-stoichiometric AB2 alloys. *J. Alloys Compd.* **2004**, *381*, 140–150, doi:10.1016/j.jallcom.2004.03.081.

47. M. Kandavel, S. R. The effect of non-stoichiometry on the hydrogen storage properties of Ti-substituted AB 2 alloys. *J. Phys. Condens. Matter* **2003**, *15*, 7501–7517.

48. Sandrock, G. A panoramic overview of hydrogen storage alloys from a gas reaction point of view. *J. Alloys Compd.* **1999**, *293–295*, 877–888, doi:10.1016/S0925-8388(99)00384-9.

49. Ivey, D. G.; Northwood, D. O. Storing energy in metal hydrides: a review of the physical metallurgy. *J. Mater. Sci.* **1983**, *18*, 321–347, doi:10.1007/BF00560621.

50. Nakamura, Y.; Akiba, E. H ydriding properties and crystal structure of NaCl-type mono-hydrides formed from Ti–V–Mn BCC solid solutions. *J. Alloys Compd.* **2002**, *345*, 175–182.

51. Friedlmeier, G.; Manthey, A.; Wanner, M.; Groll, M. Cyclic stability of various application-relevant metal hydrides. *J. Alloys Compd.* **1995**, *231*, 880–887, doi:10.1016/0925-8388(95)01776-3.

52. Young, K.; Ouchi, T.; Yang, J.; Fetcenko, M. A. Studies of off-stoichiometric AB2 metal hydride alloy: Part 1. Structural characteristics. *Int. J. Hydrogen Energy* **2011**, *36*, 11137–11145, doi:10.1016/j.ijhydene.2011.05.057.

53. Young, K.; Nei, J.; Huang, B.; Fetcenko, M. A. Studies of off-stoichiometric AB2 metal hydride alloy: Part 2. Hydrogen storage and electrochemical properties. *Int. J. Hydrogen Energy* **2011**, *36*, 11146–11154, doi:10.1016/j.ijhydene.2011.05.056.

54. Dornheim, M. Thermodynamics of Metal Hydrides : Tailoring Reaction Enthalpies of Hydrogen Storage Materials. *Thermodyn. - Interact. Stud. - Solids, Liq. Gases,* **2011**, *Dr. Juan C*, 891–918, doi:10.5772/21662.

55. Driessen, A.; Sanger, P.; Hemmes, H.; Griessen, R. Metal hydride formation at pressures up to 1 Mbar. *J. Phys. Condens. Matter* **1990**, *2*, 9797–9814, doi:10.1088/0953-8984/2/49/007.

56. Wang, L.; Young, K.; Nei, J.; Pawlik, D.; Ng, K. Y. S. Hydrogenation of AB5 and AB2 metal hydride alloys studied by in situ X-ray diffraction. *J. Alloys Compd.* **2014**, *616*, 300–305, doi:10.1016/j.jallcom.2014.07.125.

57. Chen, Z.; Xiao, X.; Chen, L.; Fan, X.; Liu, L.; Li, S.; Ge, H.; Wang, Q. Influence of Ti super-stoichiometry on the hydrogen storage properties of Ti1+xCr1.2Mn0.2Fe0.6 (x = 0-0.1) alloys for hybrid hydrogen storage application. *J. Alloys Compd.* **2014**, *585*, 307–311, doi:10.1016/j.jallcom.2013.09.141.

58. Chen, Z.; Xiao, X.; Chen, L.; Fan, X.; Liu, L.; Li, S.; Ge, H.; Wang, Q. Development of Ti-Cr-Mn-Fe based alloys with high hydrogen desorption pressures for hybrid hydrogen storage vessel application. *Int. J. Hydrogen Energy* **2013**, *38*, 12803–12810, doi:10.1016/j.ijhydene.2013.07.073.

59. Ivey, D. G.; Chittim, R. I.; Chittim, K. J.; Northwood, D. O. Metal hydrides for energy storage. *J. Mater. Energy Syst.* **1981**, *3*, 3–19, doi:10.1007/BF02833316.

60. Westlake, D. G. Hydrides of intermetallic compounds: A review of stabilities, stoichiometries and preferred hydrogen sites. *J. Less-Common Met.* **1983**, *91*, 1–20, doi:10.1016/0022-5088(83)90091-7.

61. Flanagan, T. B.; Bowerman, B. S.; Biehl, G. E. Hysteresis in metal/hydrogen systems. *Scr. Metall.* **1980**, *14*, 443–447.

Figures:

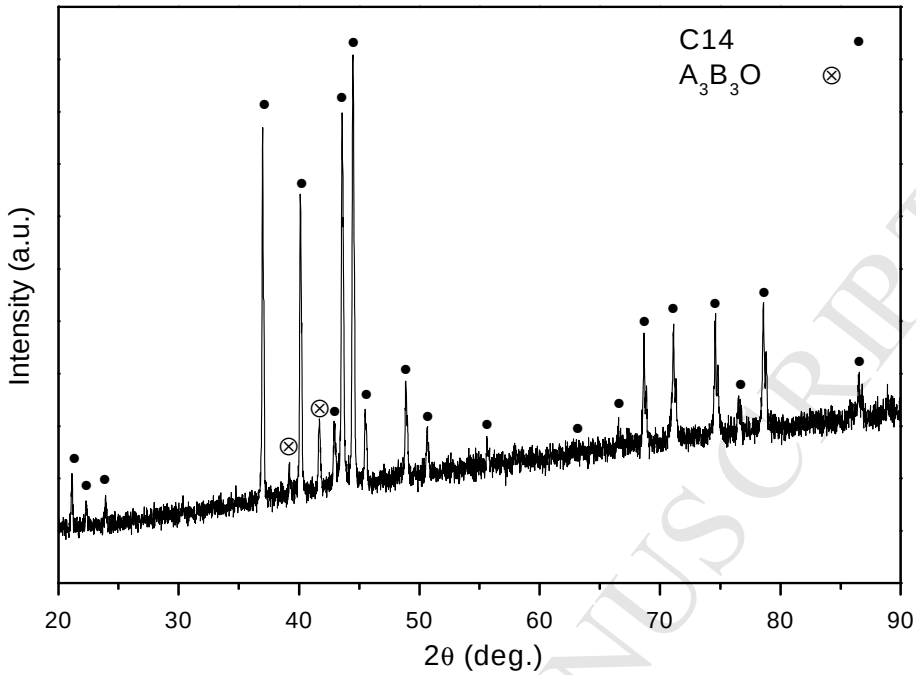

Figure 1: XRD pattern of the as-received Ti-Mn based alloy (Alloy 1).

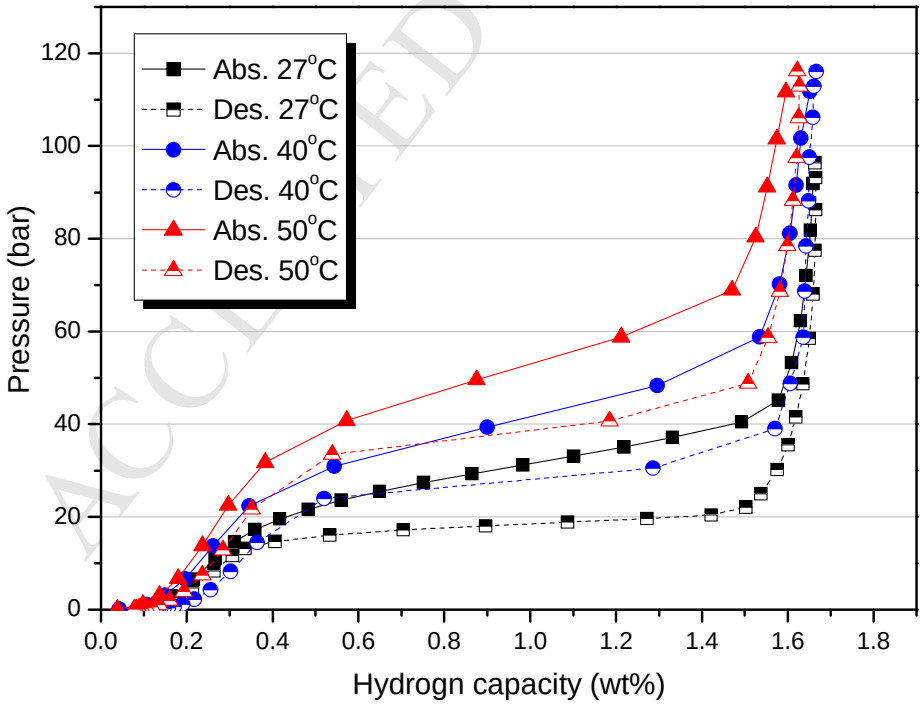

Figure 2: PCI curves of the as-received Ti-Mn based alloy (Alloy 1), showing hydrogen

absorption (solid symbols) and desorption (half-filled symbols) at different temperatures.

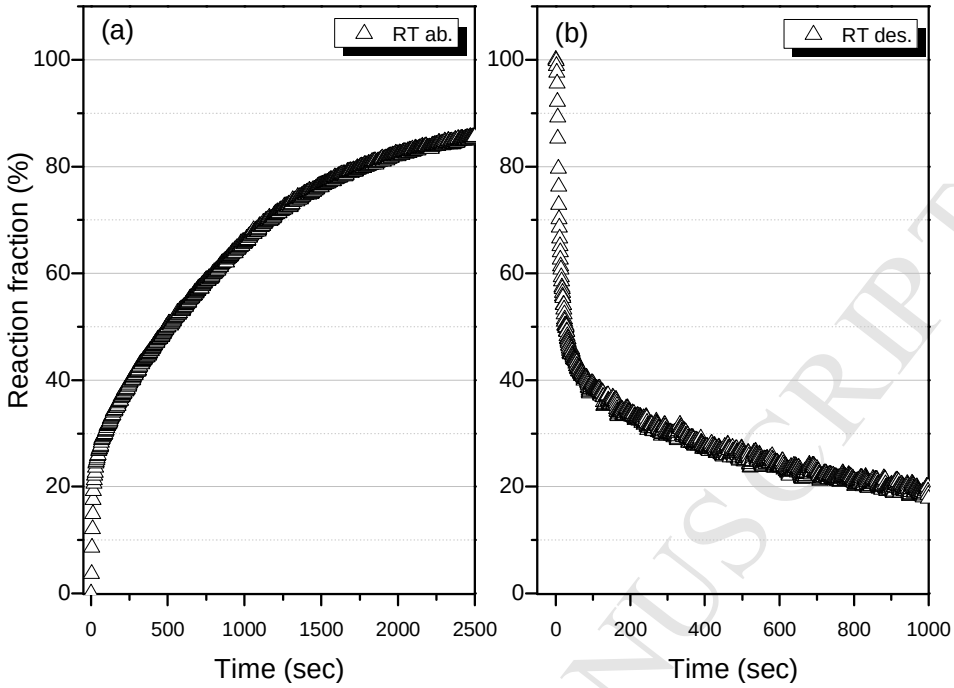

Figure 3: Hydrogen absorption (a) and desorption (b) curves of the as-received Ti-Mn based alloy (Alloy 1)

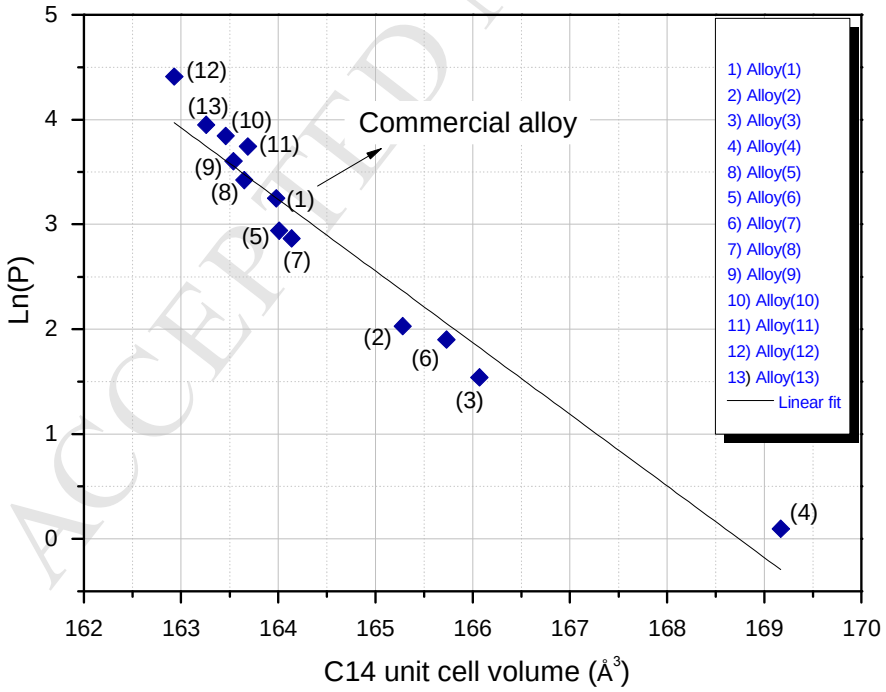

Figure 4: Relationship between the C14 Laves phase unit cell volume and the plateau pressure of the studied alloys.

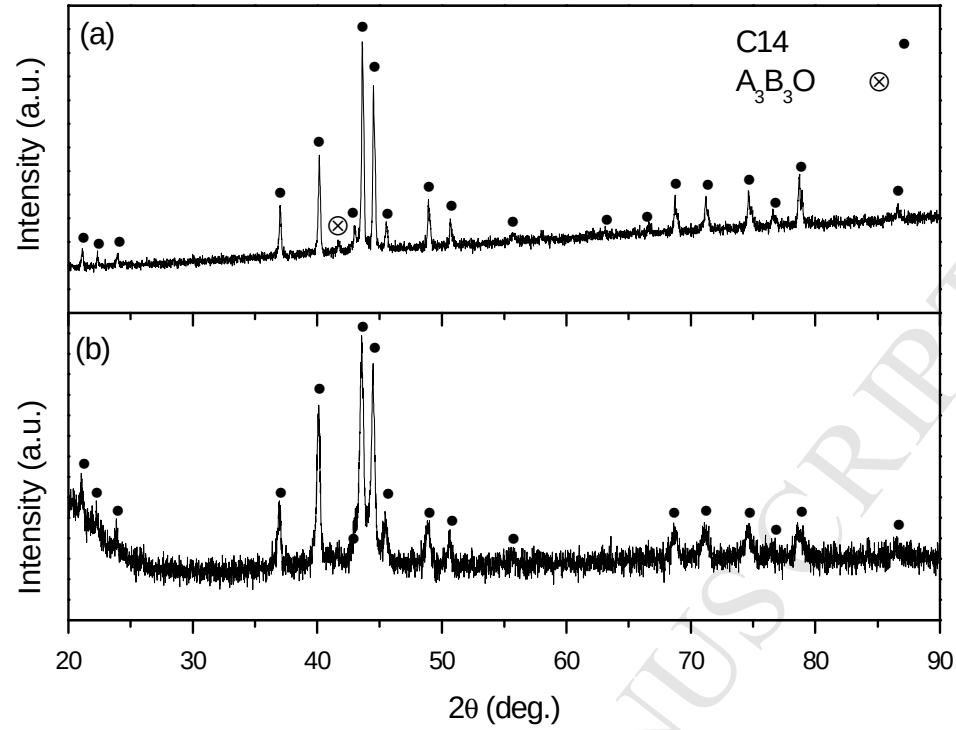

Figure 5: XRD patterns of the Alloy 14 after fabrication from elements (a) and after 1007 hydrogen absorption/desorption cycles.

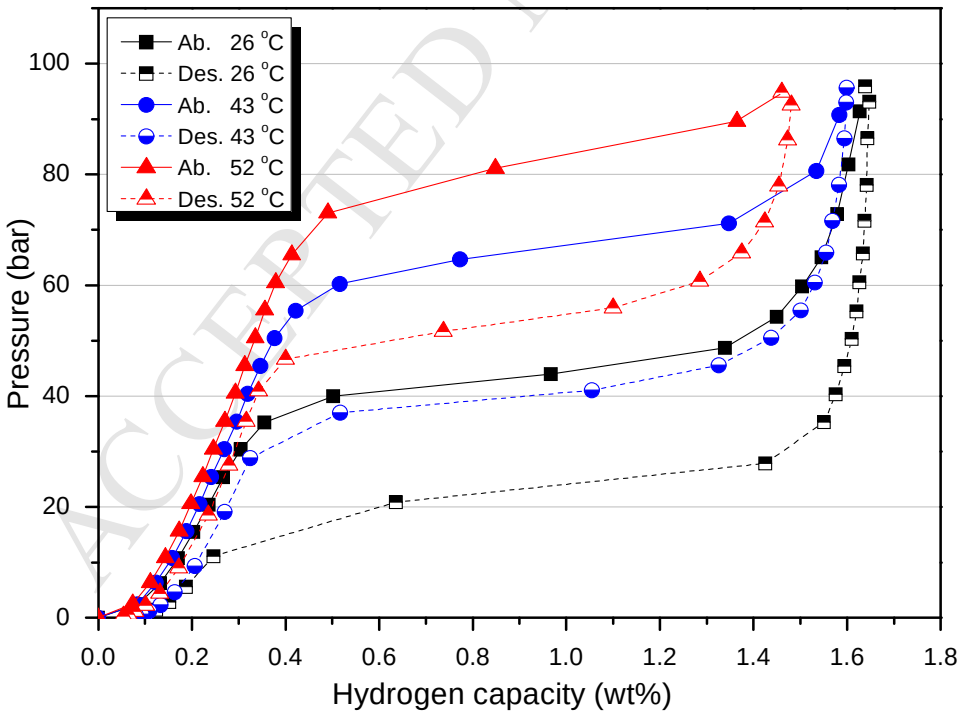

Figure 6: PCI curves of the Alloy14 showing hydrogen absorption (solid symbols) and desorption (half-filled symbols) at different temperatures.

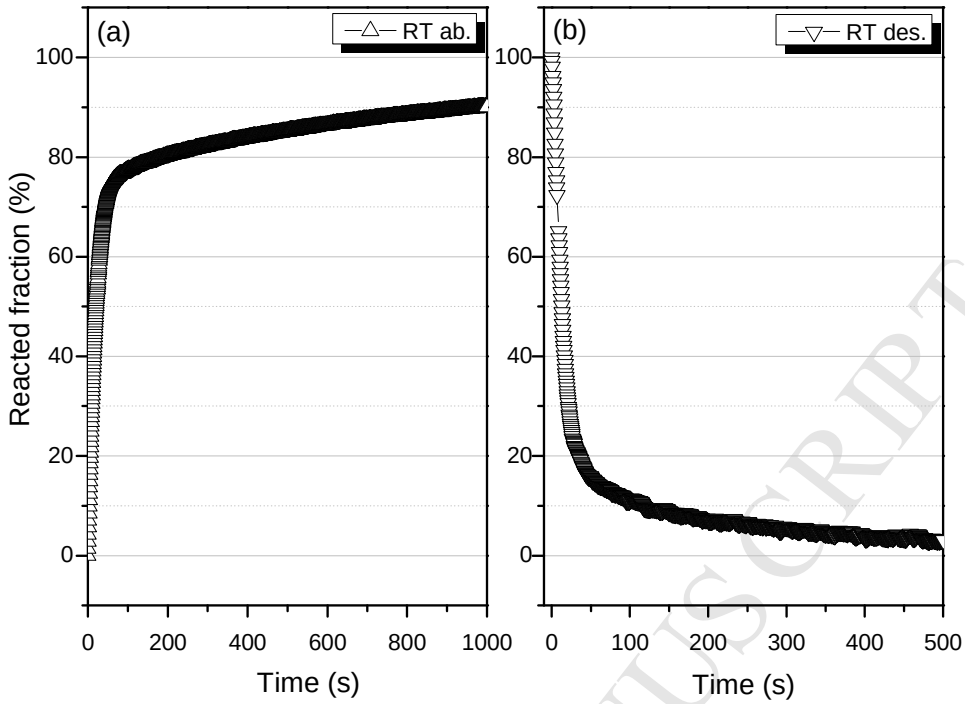

Figure 7: Hydrogen absorption (a) and desorption (b) curves of the Alloy 14

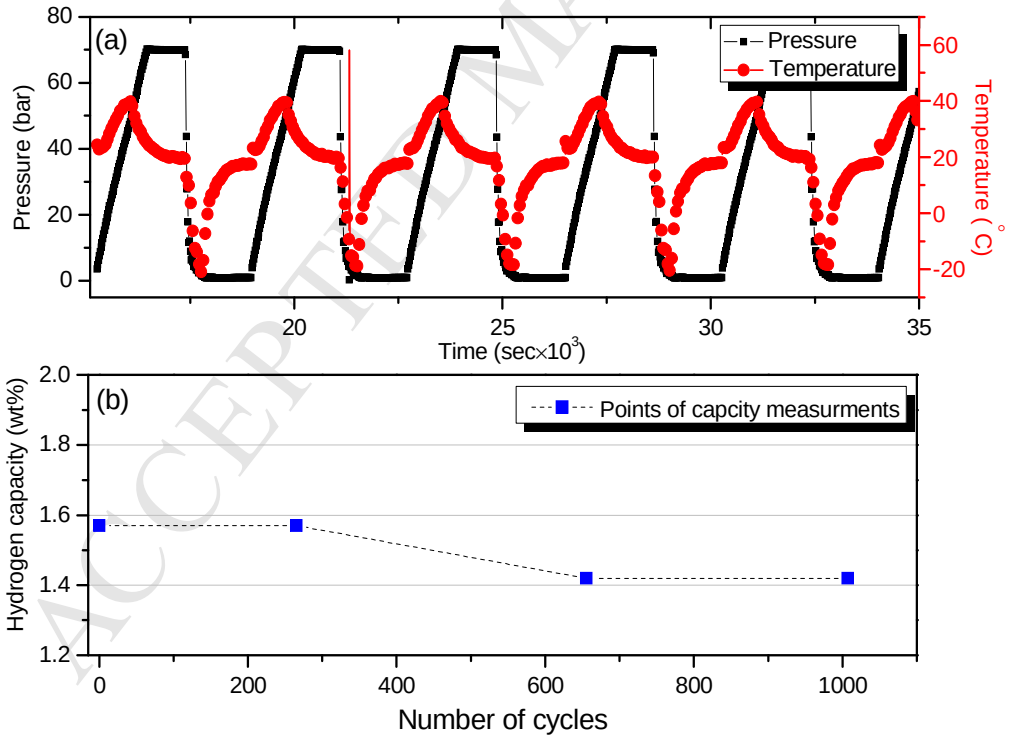

Figure 8: (a) shows a few room temperature cycles of the hydrogen absorption and desorption performed at 70 and 0.5 bar. A complete hydrogen absorption and desorption is considered as a cycle, accompanied by exo/endothermic heat profile of the sample. (b) is

hydrogen capacity of the Alloy 14 as a function of cyclic hydrogen absorption/desorption (dash line is a guide to the eye) measured in-situ at specific points.

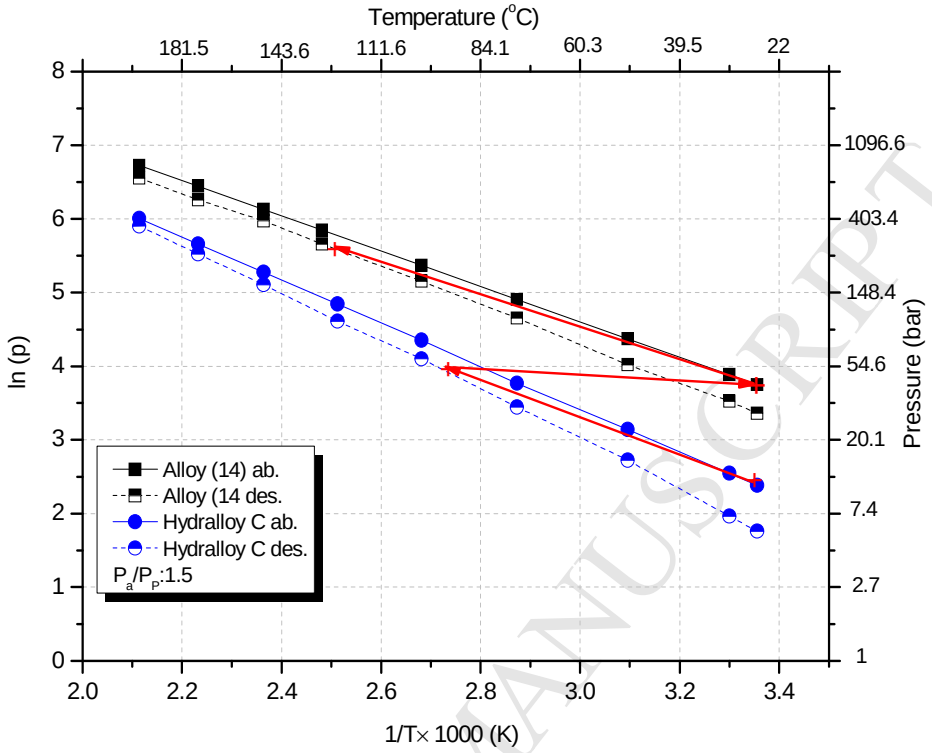

Figure 9: The Estimated operational condition of the Alloy 14 when combined with a low-pressure alloy (Hydralloy C), calculated by the van't Hoff equation. Red arrows show the operation steps, *i.e.* (1) hydrogen absorption and desorption at the low pressure stage, (2) admittance of hydrogen that is 1.5 times higher than the plateau pressure of the Alloy 14, achieved by increasing the low stage temperature, and (3) compressing hydrogen above 350 bar by increasing the high stage temperature to 130 °C.

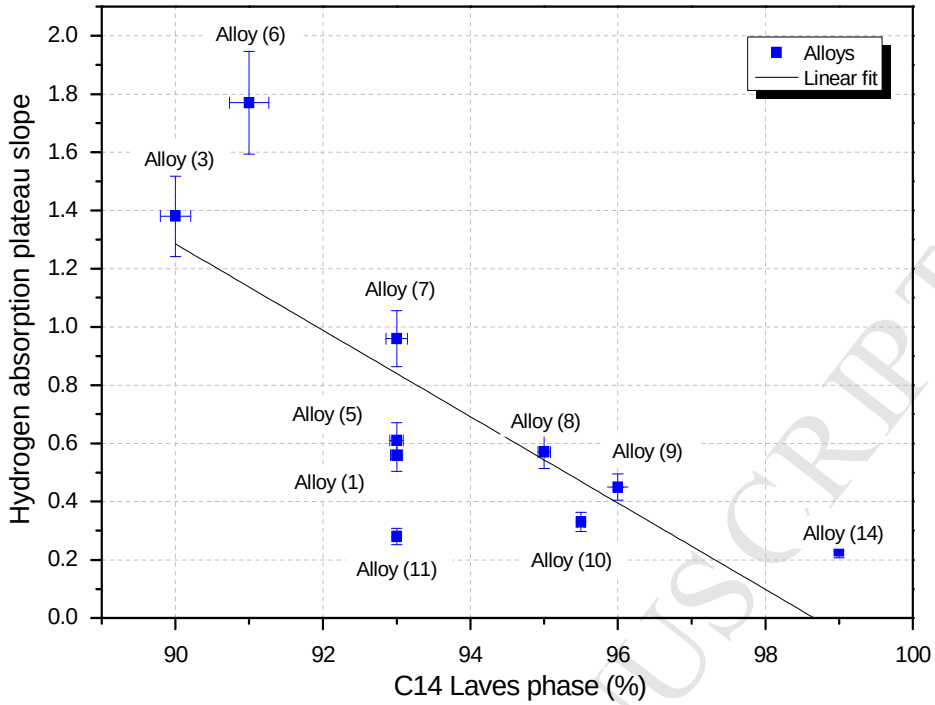

Figure 10: Changes in the hydrogen absorption plateau slope of the studied alloys according to the C14 Laves phase content of the alloys.

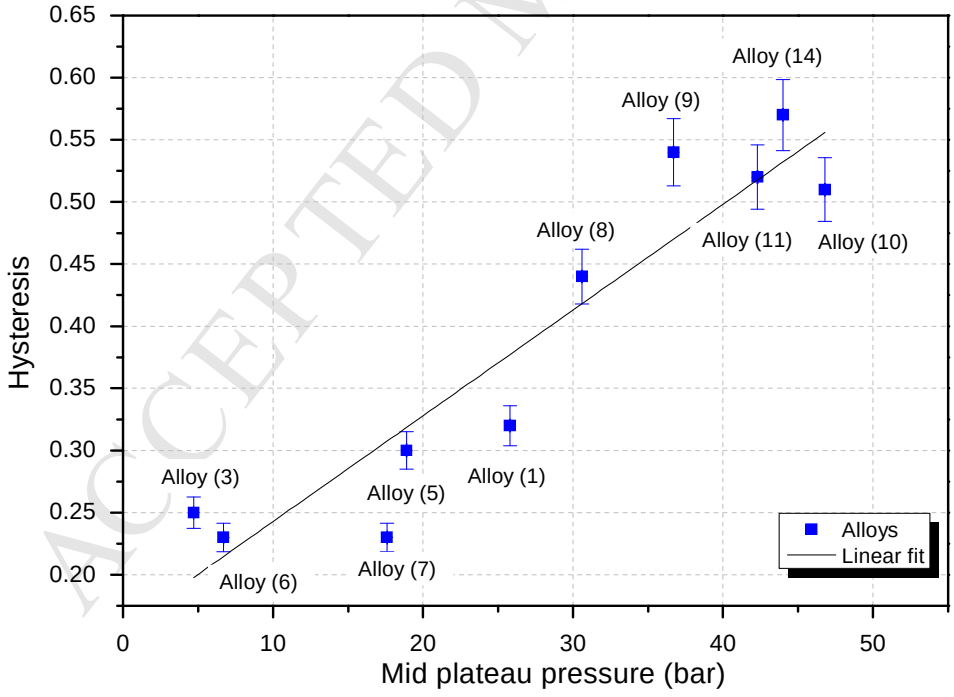

Figure 11: Changes in the level of hysteresis as a function of mid plateau pressures of the studied alloys.

Tables:

Table 1: Compositional modification of the as-received Ti-Mn based alloy. Included are compositional analyses of the modified alloys obtained by EDS (with an average error of ± 2%), B/A atomic ratio, phase abundance (%) and the C14 Laves phase unit cell volume.

Sample	Added elements (g) to 2g of the as-received alloy						EDS composition (at. %)	B:A atomic ratio	Phase abundance (%)			C14 cell volume (Å^3)
	Ti	V	Mn	Ni	Cr	Fe			C14	BCC	A_3B_3O	
Alloy 1							$Ti_{33}V_{13.1}Mn_{47.7}(Zr_{1.2}Cr_{1.4}Fe_{3.5})$	1.92	93		7	163.95
Alloy 2		0.2					$Ti_{31.3}V_{23.2}Mn_{40.5}(Zr_{0.75}Cr_{1.3}Fe_{2.2})$	2.09	82	9	9	165.28
Alloy 3	0.1	0.1					$Ti_{34.9}V_{17.3}Mn_{42.5}(Zr_{0.6}Cr_{1.4}Fe_{3.2})$	1.81	90		10	166.07
Alloy 4	0.4	0.8					$Ti_{34.5}V_{33.9}Mn_{28.5}(Zr_{0.5}Cr_{0.9}Fe_2)$	1.86	73	15	12	169.17
Alloy 5				0.05			$Ti_{32}V_{14}Mn_{46.8}Ni_{6.1}(Zr_{0.7}\ Cr_{1.2}Fe_{3.2})$	2.09	93		7	164.01
Alloy 6					0.05		$Ti_{32.9}V_{15.8}Mn_{43}(Zr_{0.7}Cr_{1.7}Fe_{3.4})$	1.98	91		9	165.73
Alloy 7						0.05	$Ti_{33.3}V_{15..3}Mn_{44.1}(Zr_{0.6}Cr_{1.6}Fe_{4.9})$	1.94	93		7	164.13
Alloy 8			0.1				$Ti_{30.5}V_{14.7}Mn_{49.3}(Zr_{0.6}Cr_{1.4}Fe_{3.2})$	2.2	95		5	163.65
Alloy 9			0.15				$Ti_{31.3}V_{13.2}Mn_{50.1}(Zr_{0.7}Cr_{1.4}Fe_3)$	2.11	96		4	163.54
Alloy 10			0.15		0.05		$Ti_{28.6}V_{11.1}Mn_{50.9}(Zr_{0.7}Cr_{4.5}Fe_{4.1})$	2.4	95.5		4.5	163.46
Alloy 11		0.05	0.15				$Ti_{31.4}V_{15.2}Mn_{48.1}(Zr_{0.5}Cr_{1.3}Fe_{3.3})$	2.12	93		7	163.69
Alloy 12			0.15	0.05			$Ti_{26.7}V_{12.2}Mn_{53.3}Ni_{1.6}\ (Zr_{0.6}\ Cr_{1.7}Fe_{3.6})$	2.64	82		18	162.93
Alloy 13			0.1	0.05			$Ti_{30.9}V_{12.8}Mn_{48.5}Ni_{2.1}\ (Zr_{0.6}\ Cr_{1.5}Fe_{3.3})$	2.16	94		6	163.26
Synthesised from elements Alloy 14							$Ti_{30}V_{15.8}Mn_{49.4}(Zr_{0.5}Cr_{1.1}Fe_{2.9})$	2.26	~99		~1	163.5

Table 2: Thermodynamic, kinetic and PCI characteristics of the as-received and modified alloys.

Sample	P_{ab} (mid plateau, 23 °C)	ΔH des. (kJ/mol H_2)	ΔS des. (J/Kmol)	H capacity (wt%, @90 bar)	Hysteresis (ln(Pa/Pd), RT)	Slope d(lnP)/d(wt%)	Ab. Kinetic (80%, min)
Alloy 1	25.8 (27 °C)	25.8	110	1.65	0.32	0.67	29
Alloy 2	7.6	27.2	105.9	1.66	0.28	1.03	23
Alloy 3	4.7	29.9	110.2	1.32	0.25	2.19	12
Alloy 4	1.1	32.7	99.2	1.76	-	-	17
Alloy 5	18.9	26.3	111.1	1.64	0.30	0.7	9
Alloy 6	6.7 (21 °C)	27.8	108.5	1.59	0.23	1.77	11
Alloy 7	17.6 (25 °C)	28.7	118.5	1.3	0.23	0.96	17
Alloy 8	30.6 (21 °C)	24.2	107.1	1.52	0.44	0.57	13
Alloy 9	36.7	24.7	109.3	1.53	0.54	0.45	2
Alloy 10	46.8 (24 °C)	24.8	111.3	1.39	0.51	0.33	3
Alloy 11	42.3 (27 °C)	24	107.8	1.35	0.52	0.28	3
Alloy 12	>70	-	-	-	-	-	-
Alloy 13	52 (26 °C)	-	-	1.37	0.6	-	2
Synthesised from elements Alloy 14	44 (26 °C)	24.3	109.5	1.6	0.57	0.23	3

Highlights

- A high-pressure hydrogen storage Ti-Mn based alloy was developed for hydrogen compression.
- Thermodynamics and kinetics of the alloy were tailored by the compositional modification
- Key parameters controlling the hydrogen absorption plateau slope and hysteresis are discussed.
- Hydrogen storage properties of the developed alloy remained almost constant after 1000 cycles.